Differential Doppler Velocity: A Radar Parameter for Characterizing Hydrometeor Size Distributions

DAMIAN R. WILSON,* ANTHONY J. ILLINGWORTH, AND T. MARK BLACKMAN

JCMM, Department of Meteorology, University of Reading, Reading, United Kingdom

(Manuscript received 18 March 1996, in final form 15 October 1996)

ABSTRACT

Observations of Doppler-resolved spectra of differential radar reflectivity provide estimates of particle shapes as a function of their terminal velocity, and they can be derived by having the antenna at a significant elevation angle. Turbulence tends to smear out the details of the actual spectra observed, but the difference in the mean values of velocity using horizontal and vertical polarizations, which the authors call the ''differential Doppler velocity'' (DDV), is unaffected. Larger raindrops fall faster and are oblate, so values of DDV are positive. If a gamma function is used for the raindrop size spectrum, then the observed DDV and Z_{DR} correspond to particular values of median drop diameter D_0 and the dispersion index m. The scaling parameter N_0 is derived from Z. Estimates of m have a mean value of 5 but vary substantially. An error in rainfall rate of up to $\pm 15\%$ results if the rainfall rate is computed from Z and Z_{DR} alone, and m is assumed constant at 5. An overestimation of more than 30% occurs if m is assumed to be 0. DDV values in stratiform ice are slightly negative. The values in ice are explicable in terms of a mixture of slowly falling oblate crystals and faster-falling spherical aggregates. In the bright band, DDV is consistent with the coexistence of oblate snowflakes and faster-falling raindrops.

1. Introduction

Marshall and Palmer (1948) fitted observed raindrop size distributions to an exponential. More recently (e.g., Ulbrich 1983), a gamma function of the form

$$N(D) = N_0 D^m \exp\left[-\frac{(3.67 + m)D}{D_0}\right] \qquad (1)$$

has been used with three free parameters, N_0, D_0, and m. This reduces to a two-parameter (N_0 and D_0) exponential if m, the dispersion parameter, is fixed at zero. The overall scaling parameter N_0 and the median drop size D_0 can be fitted to observations of the reflectivity Z and the differential reflectivity Z_{DR}. The problem for measurements made solely using radar is that after Z and Z_{DR} have been considered there is no obvious choice of a third radar parameter, which is required to fit the gamma distribution. Work has been previously performed by using Z, Z_{DR}, and a rainfall rate from a gauge as a third parameter, but this suffers from the fact that the radar and the gauge have different sampling volumes. Ulbrich and Atlas (1984) used distrometer data alone to calculate values of Z, Z_{DR}, and rainfall rate as the three ''observations'' and found they were consistent with $m = 2$. However, the truncation of the large drops in the spectrum due to poor measurement by the distrometer artificially raises the value of m, and hence this estimate may be too high. Goddard and Cherry (1984) suggest that $m = 5$ in the gamma distribution removes the bias between distrometer-measured rainfall rates and rainfall rates calculated from the Z and Z_{DR} inferred from the distrometer spectra. They also compared radar measurements with rain gauges and observed that the bias and scatter of the rainfall rates from rain gauge and radar (from Z and Z_{DR}) were much reduced when they considered $m = 5$ rather than $m = 0$. Ulbrich (1983) investigated the possibility of deriving a relationship between m and the other parameters in the drop size distribution by analyzing published empirical reflectivity rainfall rate relationships. The idea was that a given reflectivity rain-rate relationship can be considered as being due to a gamma distribution, assuming that m and N_0 are constants and are determined from the values a and b in the relationship $Z = aR^b$. Variations in D_0 account for different rainfall rates. Since the units of N_0 depend upon the value of m used, a relationship between N_0 and m is to be expected. However, each m and the corresponding N_0 are derived by assuming that D_0 is the only quantity varying in each of the Z–R relationships. This is inconsistent with trying to derive a relationship between the changing parameters of N_0 and m.

*Current affiliation: Hadley Centre, Meteorological Office, Bracknell, United Kingdom.

Corresponding author address: Dr. Anthony J. Illingworth, Dept. of Meteorology, University of Reading, 2 Earley Gate, P.O. Box 239, Whiteknights, Reading RG6 6BB, United Kingdom.
E-mail: A.J.Illingworth@reading.ac.uk

This paper investigates the use of a Dopplerized dual-polarization radar for obtaining a third measurement, in order to fit a gamma drop size distribution, by examining the difference in Doppler velocities measured at horizontal and vertical polarization when a radar observes at an elevation angle significantly above the horizontal. The difference in velocities is found to be sensitive to m. A linear dual-polarization Doppler radar usually measures mean polarization characteristics of a precipitation volume, such as Z_{DR}, at low elevation or, by pointing vertically, the mean fall velocity of the precipitation. If a radar observes at an elevation angle that is significantly above the horizontal, say 30°, then a component of the fall velocity of the particles is toward the radar, and it hence contributes to the Doppler velocity of the target. Additionally, measurements of Z_{DR} can be made and corrected for the elevation angle.

Russchenberg (1993) has fitted a three-parameter drop size distribution to radar observations of the reflectivity Z, the differential reflectivity Z_{DR}, and the variance of the Doppler spectrum, assuming that the spectrum is broadened by the spread of fall speeds. The technique of Russchenberg, although accurate in theory, fails when any other mechanism exists for widening the Doppler spectrum of the target, such as wind shear or isotropic turbulence. It is our experience that such broadening mechanisms are common and difficult to estimate. Shear or turbulence will always increase the width of the Doppler spectrum, hence producing a bias in results even when their contributions are smaller than that of the broadening due to the spread of fall speeds. It is therefore desirable to find a technique that is unaffected by, or at least unbiased by, broadening mechanisms.

2. Differential Doppler velocity

The technique we consider is similar to that used by Metcalf (1986), who analyzed the difference in various Doppler velocities measured using circular polarization. He was able to estimate, among other things, whether the particles that were most aligned had larger or smaller Doppler velocities than the mean. Metcalf concentrated on viewing precipitation near horizontal incidence and looking for the effect of high wind shears, which will be seen in section 3 to affect the Doppler velocities of different fall speeds of particles. He also pointed out that at high elevations the difference in Doppler velocities between particles due to fall speed differences should be greater than those induced by shear. Hence, information about whether the most aligned particles are falling faster or slower than the mean is available.

In this paper, we look at the difference in Doppler velocities measured with a linear dual-polarization Doppler radar. The technique is to observe at an elevation angle from around 10° to 40° and to investigate the difference in the mean Doppler velocities measured with horizontal polarization v_H and vertical polarization v_V. As an example to show what is expected, consider the case of rain in the absence of any wind. Here, the larger particles fall faster than the smaller particles and also are the most eccentric in shape, so they have a larger value of Z_{DR}. Since one is interested in an interpretation in terms of fall velocities, when the target is moving toward the radar, the Doppler velocity will be defined as positive (this is the opposite of the usual definition). An estimate of the Doppler velocity made in the horizontal polarization will be greater than a similar estimate made in the vertical polarization. The larger drops, which are falling faster, contribute more to the mean value of Doppler velocity in the horizontal polarization than they do in the vertical. Figure 1 pictorially demonstrates the basis of the mechanism for rain, the solid line representing the reflectivity-weighted mean fall velocity in the horizontal polarization and the dashed line the mean for the vertical. It is clear that the actual Doppler velocity difference $v_H - v_V$ will vary with elevation angle θ; the larger the angle, the larger the component of fall velocities contributing to the Doppler velocity. The component is proportional to $\sin\theta$, so a measure of the ''differential Doppler velocity'' (DDV) is defined as

$$\text{DDV} = \frac{v_H - v_V}{\sin\theta}. \tag{2}$$

Since DDV has been adjusted (by the $\sin\theta$ term) to the situation in which the fall velocities are effectively viewed at vertical incidence, one should more accurately call DDV ''DDV at vertical incidence.'' This does not

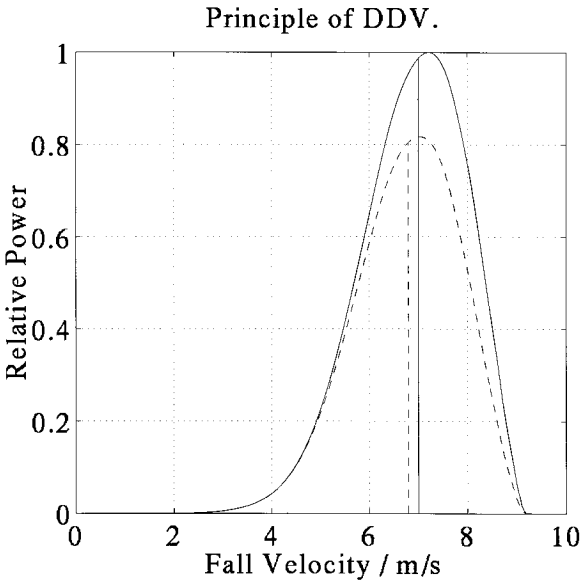

FIG. 1. A schematic spectrum in rain of power against fall speed for horizontal polarization (solid) and vertical polarization (dashed). The vertical lines represent the mean fall velocities. The faster-falling particles have higher values of Z_{DR}, so the mean Doppler velocity in the horizontal polarization is greater than that for the vertical polarization.

imply that the radar measurements shown are performed with the radar vertical, but that the $\sin\theta$ adjustment has been made. All the values shown in this paper have the adjustment applied. DDV should therefore be a constant for a particular target and independent of viewing angle. It measures, in effect, the way Z_{DR} varies with fall velocity. For high elevations, the Z_{DR} of each particle will be reduced; hence, the measured DDV is not quite a constant with θ. The obvious example is that $v_H = v_V$ when the radar views vertically. An adjustment is desirable for this effect, although it will be shown later that this is not simple. For small elevation angles, there is little difficulty, and the measured DDV is defined as in (2) throughout the rest of this paper. Figure 1 shows that DDV is significantly smaller than the overall spread of the Doppler velocities, and this should be remembered in the interpretation of the following results.

As air pressure decreases, the fall speed of a particle increases. The particles are assumed to fall at their terminal fall speed, which Pruppacher and Klett (1978) show can be written approximately as

$$v_t = v_{t0}\left(\frac{\rho_0}{\rho}\right)^{0.4}, \tag{3}$$

where v_t is the fall speed corresponding to air density ρ, and v_{t0} and ρ_0 are the terminal velocities and density at a reference level (usually sea level). Since this expression modifies all fall velocities by a constant factor for a given height, one can simply adjust measured DDV values to sea level by dividing by the factor $(\rho_0/\rho)^{0.4}$. Pruppacher and Klett (1978) also show that the exponent is not truly a constant, but varies slightly with the diameter of the particle. However, this is a negligible change compared to the observational errors of the measurements that will be presented later. For example, the correction introduced by using (3) is 1.082 at 2-km altitude and 1.281 at 6-km altitude. This modification is also necessary in precipitation other than rain, such as the melting layer and ice, and the data presented here have all been adjusted for the changing fall speeds.

The measurements that we consider here were all performed using the Chilbolton multiparameter Doppler radar, situated in Hampshire, United Kingdom. It has a fully steerable 25-m-diameter dish, with a wavelength of 10 cm (S band), giving a beam width of 0.25°. The transmission is alternately horizontally and vertically linearly polarized, with a pulse repetition frequency between two pulses of the same polarization of 305 Hz. Reception is at both horizontal and vertical polarization for each pulse. The pulse length is 0.5 μs, so a single gate length is 75 m.

a. Estimation

DDV is measured by subtracting the estimate of the Doppler velocity in the vertical polarization v_V from the estimate of v_H and modifying the result as discussed above. Both v_H and v_V can be separately estimated by the standard method of pulse pairs described by Doviak and Zrnić (1984). Here, v_H is estimated as

$$\hat{v}_H = -\left(\frac{\lambda}{4\pi T_s}\right)\arg\sum_n H_n H_{n+1}^*, \tag{4}$$

where H_n is the complex amplitude returned by the nth transmitted pulse of horizontal polarization, T_s is the time between successive pulses of horizontal polarization, and λ is the wavelength of the radar. A similar equation yields v_V for vertically polarized pulses. Another method of velocity estimation is to use a pulse pair method but to weight all the pulses by the same amount (the ''phase-only'' estimator), rather than applying more weight to the pulses with the largest amplitude. This estimator, which can be calculated if one measures only phase rather than both amplitude and phase information, is therefore

$$\hat{v}_h = -\left(\frac{\lambda}{4\pi T_s}\right)\arg\sum_n \frac{H_n H_{n+1}^*}{|H_n||H_{n+1}^*|}. \tag{5}$$

It is possible to simulate time series for rain by allowing several drops of different sizes to fall at their terminal velocities, their different fall speeds (when viewed from a high elevation angle) causing decorrelation of the calculated received radar amplitude with time. No other decorrelation mechanism is considered. A set of such simulations, displayed in Fig. 2, shows that the pulse pair estimator has around two and a half times less

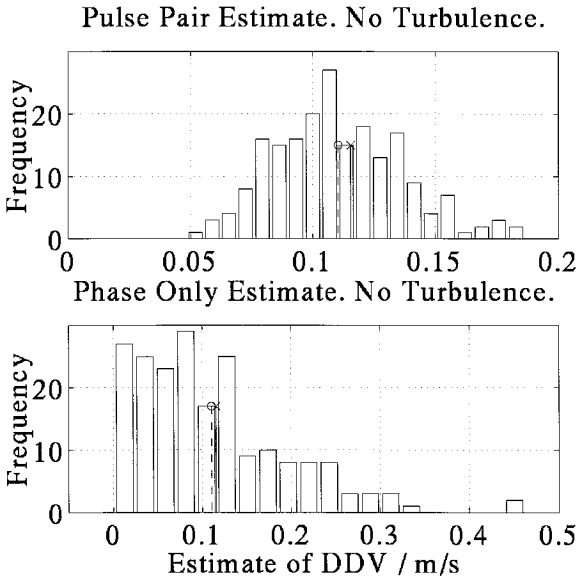

FIG. 2. A distribution of estimates of DDV from a simulation using 128 pulse-pair time series, with only fall velocities contributing to Doppler widths. The mean DDV of the estimator from the simulation is marked with a circle [from Eq. (4)]. The theoretical value [from Eq. (6)] is marked with a cross. (a) Uses the pulse-pair estimator [Eqs. (2) and (1)] and (b) uses the phase-only estimator [Eqs. (3) and (1)].

statistical error than the phase-only estimator and so should be used in preference to it. Close examination also shows that, in the case of rain (where DDV is positive), the phase-only estimator produces a mean estimate of DDV that is slightly different from the mean estimate of DDV from the pulse pair estimator. This should not be surprising since the estimators are known to estimate the mean Doppler velocity only in the case where the power–velocity spectra are symmetric; clearly, if any consistent change of Z_{DR} with fall velocity occurs (which is what DDV is measuring), then the power–velocity spectra for the horizontal and vertical polarizations cannot both be symmetric. It is therefore essential to investigate how well the estimator agrees with a theoretical interpretation of DDV.

One can define a theoretical DDV for a given distribution of particles. It is natural to assume that the measured DDV will be close to the difference in the mean velocities u_H and u_V, where u_H is the power-weighted mean fall velocity of the group of particles in the horizontal polarization. The Z_{DR} for each particle is adjusted to its value at the appropriate elevation angle (see section 2b). This can be written as

$$u_H = \frac{\sum |S_{hi}|^2 (v_i/\sin\theta)}{\sum |S_{hi}|^2}, \tag{6}$$

where $|S_{hi}|^2$ is the reflectivity of the ith particle in the horizontal polarization viewed at the measuring angle, and v_i is the Doppler velocity of the ith particle. From simulation, the theoretical DDV $u_H - u_V$ is found to be close to the measured DDV using either the pulse pair or the phase-only estimators $(v_H - v_V)/\sin\theta$, as shown in Fig. 2, although the values are not precisely equal. The statistical error on the measurements discussed later, however, is seen to be significantly greater than the differences between the two estimates of DDV [from (4) and (5)] and the theoretical DDV [from (6)]. Subsequently, they are assumed to be equal to each other with little error.

b. *Adjustment to DDV due to Z_{DR} varying with elevation angle*

The theoretical DDV can be easily deduced using Z_{DR} values that are applicable for a radar beam at a 0° elevation angle and fall velocities that are applicable at a 90° elevation angle. Clearly, this hypothetical case cannot be measured directly, but it is a useful way to express measured values of DDV. The $\sin\theta$ correction [(2)] adjusts the measured Doppler velocity difference $v_H - v_V$, but an additional correction is required due to the fact that Z_{DR} values are measured at a finite elevation angle. As the elevation angle increases, Z_H tends to remain fairly constant but Z_V increases, approaching the value of Z_H at vertical incidence. The measured Doppler velocity difference will tend to zero as the elevation angle increases. If there are many particles present with different Z_{DR} values and fall velocities, and only the mean Z_{DR} of the ensemble can be observed, then it is difficult to correct the measured v_H and v_V for elevation angle. However, in a theoretical calculation, the values of Z_{DR} for each particle are known, and what they would be at various high elevation angles can easily be predicted. Hence, a theoretical DDV can be simply calculated and compared directly to the measured DDV [given in (2)] using the Doppler velocities that would be measured at a 90° elevation angle and Z_{DR} at the actual measurement angle. Measurements of DDV at two different elevation angles are therefore not directly comparable, but the difference between them is often only small. The comparisons between theory and measurement shown later are all performed in this way.

3. The effect of wind

A uniform wind will have no effect upon the measurement of DDV since DDV represents a velocity difference between two estimates of Doppler velocity that are both affected by the same amount due to a uniform wind. The situation that needs to be considered is that in which there is a shear or turbulence within the pulse resolution volume. This can cause significant broadening of the Doppler spectrum.

For turbulence, where there is a distribution of Doppler velocities for each particular fall velocity, there should be no effect on the expected value of DDV; although the power–velocity distribution may be smeared out, the mean velocity remains the same and hence so should DDV. This is proved mathematically in the appendix, where turbulence can be considered as a convolution of the power spectrum. This is a powerful advantage of DDV over the observed Doppler width used by Russchenberg (1993). In order to test the effect of turbulence in the simulations described in section 2a, a random Doppler velocity change was applied to each particle. The results indicate an increase in the statistical width of the estimated DDV, but even for large turbulence levels there appears to be no, or very little, bias in the simulated DDV compared with theoretical prediction. Figure 3 displays the same situation as in Fig. 2 but with ± 2 m s^{-1} turbulence applied to each particle. Hence, it is concluded that turbulence (which need not be isotropic) has no effect on the expected value of DDV.

There are two reasons why shear should be considered as a biasing mechanism for DDV. First, if shear exists together with a change in the type of particle across the pulse resolution volume, which could occur, for example, at the bottom of the melting layer, then the measured DDV values could be biased. If high-Z_{DR} particles exist in the top half of the pulse resolution volume with large Doppler velocities toward the radar (due to the horizontal wind) and low-Z_{DR} particles at the bottom of the pulse resolution volume (where there is much less wind), then a positive DDV will be measured. This

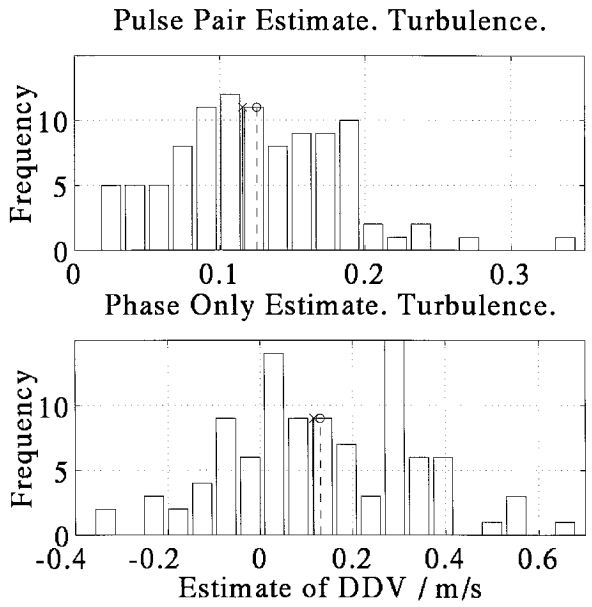

FIG. 3. A distribution of estimates of DDV from the same situation shown in Fig. 2 but with ± 2 m s^{-1} turbulence included. The distributions are wider than before. The circle marks the mean of the estimators. The cross marks the theoretical DDV. (a) Uses the pulse pair estimator and (b) uses the phase-only estimator.

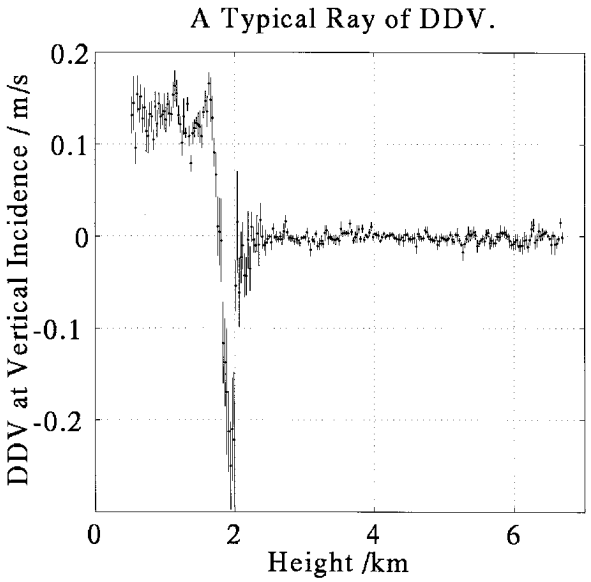

FIG. 4. A typical ray of measured DDV from a time series of 2048 pulse pairs (7 s) split into eight sections, together with empirically estimated $1\sigma_m$ errors. The elevation of the dwell was 20°.

should not be interpreted as being due to fall speeds. Obviously, the narrower the width of the beam, the less severe this problem is; the Chilbolton radar has a narrow beam width of 0.25°. Careful analysis of the data (the order of magnitude of the wind shear in a stratiform situation can be simply estimated from the change in Doppler velocity along the ray) shows that in most situations (but not all) this effect is negligible. However, one should be careful in regions where $Z_{\rm DR}$ and v_H both vary sharply.

The second reason why shear should affect DDV was identified in the investigation of Metcalf (1986). In a horizontal wind shear, the larger particles take longer to respond to the wind change, so their horizontal velocity is not that of the wind. Hence, the horizontal velocity at a given height (which will make up the greatest component of the Doppler velocity) will depend upon the fall speed of the particles. In the case where the fall speed depends upon $Z_{\rm DR}$, a bias in DDV may occur. Metcalf (1986) states the expression relating the horizontal velocity $v_{\rm horizontal}$ of a particle to the wind speed $v_{\rm wind}$, the wind shear, and the fall velocity $v_{\rm fall}$ as

$$v_{\rm horizontal} = v_{\rm wind} + \frac{v_{\rm fall}^2}{g}\left(\frac{\partial v_{\rm wind}}{\partial z}\right), \qquad (7)$$

where g is the acceleration due to gravity. The dependence upon the fall velocity squared makes this shear effect most severe at higher terminal velocities, as would occur in rain. Ice has much lower fall speeds, so even in strong wind shears this effect is negligible. This shear effect is independent of the beam width and decreases with increasing elevation angle. Ironically, it can exist only if there is some DDV present to begin with because the horizontal velocity difference depends upon the fall speeds. It will be shown later that in strong shears measurements of DDV in rain may become biased, but severe problems are not common. They reduce as the elevation angle increases because the larger component of fall speeds toward the radar swamps the difference in Doppler velocities due to horizontal velocity differences.

The great advantage of DDV is that it is independent of turbulence and, in many cases, shear. A large amount of high-quality data can be collected easily, and we are confident that the data presented in the next section are free from shear effects.

4. General results

As an introduction to the general characteristics of DDV, Fig. 4 shows values of DDV on a ray recorded with the radar dwelling at an elevation angle of around 20° and illustrates typical values not only in the rain, but in the melting layer and ice as well. One can observe that in the rain DDV is positive ($v_H > v_V$ as expected) and has a value of around 0.15 m s^{-1} (cf. Fig. 1). Within the melting layer DDV becomes negative, with a value of around -0.2 m s^{-1}, which implies that the faster-falling particles are more spherical. The negative excursion is found in all cases of stratiform precipitation, although its value can change. Within the ice, the magnitude of DDV is much less than in rain or the melting layer. This would be expected since the spread in fall velocities of ice particles is much less. Closer examination of DDV in ice shows that it is slightly negative.

Each of the three regions will be investigated in more detail below.

a. Rain

The interpretation of results in rain should be relatively simple since there exists a unique relationship between the fall velocity and shape, and hence Z_{DR}, of raindrops, and drop size distributions have been well investigated. Several plan position indicator (PPI) sections performed in stratiform precipitation with elevation angles of around 10°–20° have been studied. The melting layer is quite low in the United Kingdom, so low elevation angles are used to obtain a reasonable path length in the rain. Results are still obtainable at 10° elevation.

In order to predict DDV for various gamma functions, one needs to know (i) the fall speeds of raindrops of a given diameter, (ii) the shapes of raindrops of a given diameter, and (iii) the drop size distribution. The fall speeds we use are those of Gunn and Kinzer (1949) and the shapes those of Beard and Chuang (1987), modified by the adjustment suggested by Goddard et al. (1982), which makes small particles more spherical. The shapes are fitted by the formula

$$\frac{a}{b} = 1.075 - 0.065D - 0.0036D^2 + 0.0004D^3, \quad (8)$$

given by Poiares Baptista (1994), where a/b is the axial ratio of the oblate spheroid, D is the equivolume diameter of the particle in millimeters, and $a/b = 1$ for $D < 1.1$ mm.

Just as Z_{DR} is unaffected by the scaling parameter N_0, so DDV, being derived from mean velocities, is also independent of N_0. Hence, a plot of theoretical DDV against theoretical Z_{DR} (at a particular elevation angle) for various values of m and D_0 should indicate the expected range of measurements. For an elevation angle of just above 0°, such a diagram is shown in Fig. 5 (remember that DDV is modified by $\sin\theta$). The curved lines represent constant values of m, ranging from $m = 0$ (exponential) to $m = 11$. Since there is a large difference between the values of DDV derived from different values of m, measurements of DDV and Z_{DR} should clearly distinguish values of m.

As mentioned earlier, the change of Z_{DR} with elevation will alter the calculated DDV for different elevation angles even if the drop size distribution is the same. This effect is fairly small but worth accounting for. For example, at 15° elevation, DDV will be equal to 0.182 m s^{-1}, with $m = 2$ and $Z_{DR} = 1$ dB. At 10° elevation, DDV will be 0.186 m s^{-1}, and at 0° elevation, DDV will be 0.189 m s^{-1}. This is a change of around 4% between 0° and 15°. If DDV is set at 0.18 m s^{-1}, with $Z_{DR} = 1$ dB, then the value of m implied is 2.6 at 0° elevation, 2.3 at 10° elevation, and 2.1 at 15° elevation. Such changes will be seen later to be less than the statistical error on the observations.

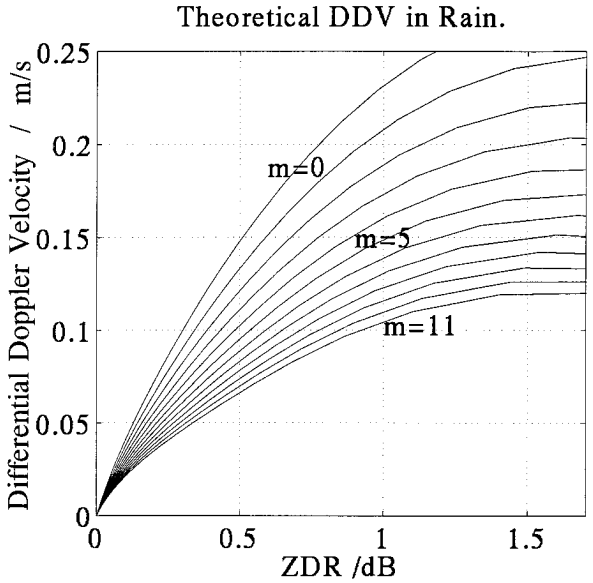

FIG. 5. The theoretical relationship between Z_{DR} and DDV for a low elevation angle. DDV has been adjusted to ''vertical incidence'' by the $\sin\theta$ correction of Eq. (2). The marked lines represent different values of m in the gamma distribution defined by Eq. (1); D_0 varies along each line.

Data from time series containing amplitude and phase information from a 10° elevation PPI were analyzed. In order to obtain an estimate of DDV with as little statistical error as possible, large areas of the PPI were averaged together to produce a single value. The averaging was performed over a section of eight gates (each gate of 75-m length) by eight rays of 256 pulse pairs each. This produced a simple mean DDV from the 64 individual estimates of DDV using the pulse-pair technique. An empirical estimate of the standard error in the mean of this value of DDV was also calculated, as well as the corresponding values of the mean and standard error of Z_{DR}. Because of the correlations between the measurements of v_H and v_V, it is difficult to theoretically calculate the error in DDV, so the empirical estimates are used. The points are plotted in Fig. 6 along with error bars for one standard error in the mean ($1\sigma_m$). The background lines are as in Fig. 5 but adjusted for $\theta = 10°$. It is clear that they do not fall along the $m = 0$ line, a value of $m = 6$ being more reasonable as a mean value of m in the gamma distribution. There also exist several points that, although having similar Z_{DR} values, have significantly different DDV values. This implies real changes in the values of m, which vary from around 2 to 11. These values are coherent in space, as shown in Fig. 6, where a line joins successive measurements in range made by averaging eight rays together and demonstrates that different regions have different m values. Figure 7 shows approximately the coherent variations of m over the whole PPI scan. The solid line in Fig. 6 represents the most northerly of the ray averages. This suggests that there is no unique re-

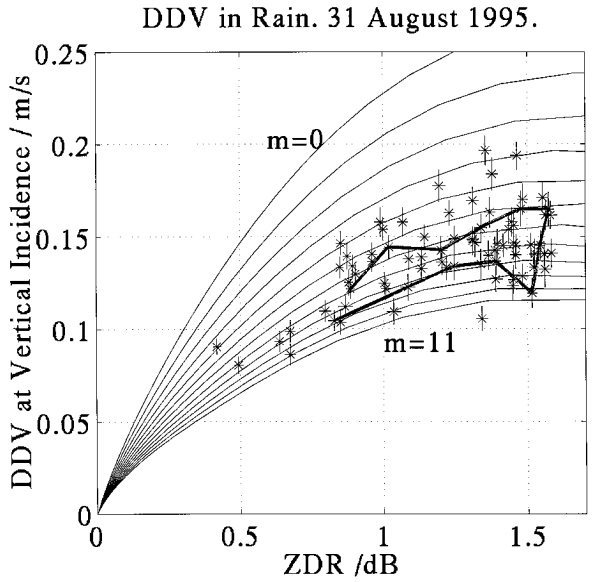

FIG. 6. Measured values of DDV and Z_{DR} in rain from a PPI at 10° elevation. The empirical $1\sigma_m$ error bars and the background of lines similar to those in Fig. 5 are also shown.

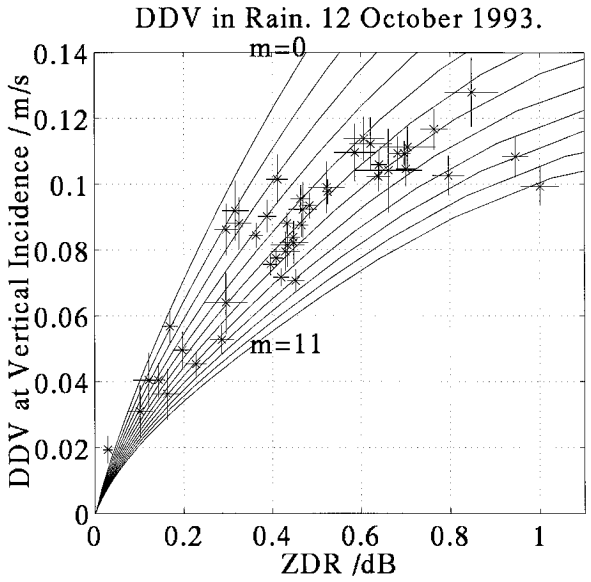

FIG. 8. A similar plot to Fig. 6 but from a PPI at 15° elevation in lighter rain. DDV and Z_{DR} values are shown along with their empirical $1\sigma_m$ errors.

lationship between Z_{DR} and DDV (or D_0 and m), which implies that a two-parameter drop size distribution (whether m is constant or a function of D_0) is not an adequate description of rainfall.

Another scan, in lighter precipitation and at 15° elevation, is displayed in Fig. 8. A similar pattern occurs with a spread of m values for a given Z_{DR}. This time $m = 5$ is a reasonable average value.

One can use the values of Z, Z_{DR}, and DDV to calculate a fit to the gamma drop size distribution defined by N_0, D_0, and m. DDV and Z_{DR} are used to fix m and D_0, and then N_0 is scaled to give the observed Z. This is shown in Fig. 9. From this, one can obtain the relationship between the reflectivity Z and the rainfall rate R, deduced from the gamma distribution fit. Figure 9 suggests rainfall rates that are around 30% lower than those calculated by presuming an exponential distri-

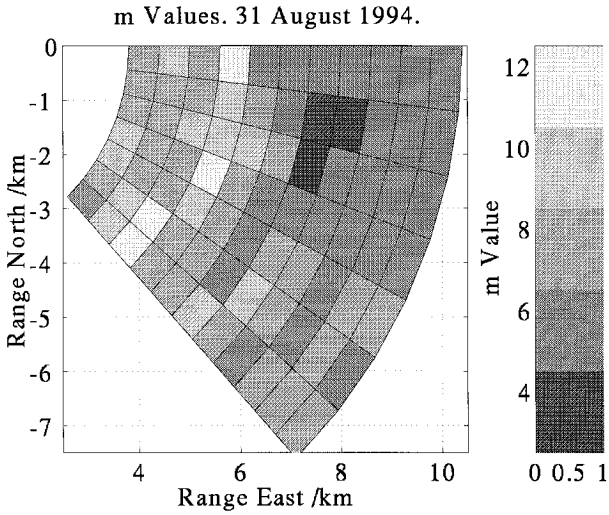

FIG. 7. The data from Fig. 6 displayed as a PPI of m values. It shows the spatial variations of m with horizontal distance.

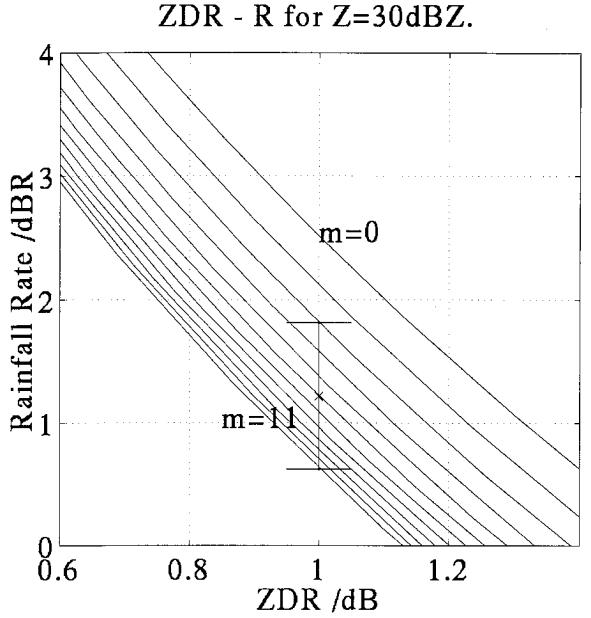

FIG. 9. A diagram to show the calculation of rainfall rate [in decibels (dB) relative to 1 mm h^{-1}] from Z_{DR} and Z for various values of m. The rainfall rate simply scales with Z, which for the diagram is considered to be 30 dBZ. The cross represents a typical value of m, deduced from the measurements of DDV, and the bar represents a typical spread in the values of m. This suggests there is a limit to how accurately the rainfall rate can be deduced from a radar.

bution that is fitted using just measurements of Z and Z_{DR}. Even if m is presumed to be a constant value of 5, there exist variations in the calculated rainfall rate for a given Z of around 15%. This is a fundamental limitation on the accuracy of radar for measuring rainfall rates. Goddard and Cherry (1984) found, using distrometer measurements, that when m was presumed to be equal to 5, there was a scatter of 14% between the distrometer-measured rainfall rate and a rate calculated from the distrometer-derived Z and Z_{DR}. Additionally, using $m = 0$ produced a bias on the order of 35%. The Goddard and Cherry (1984) results agree very well with the results presented here. Ulbrich and Atlas (1984) repeated Goddard and Cherry's analysis for their distrometer data and found that the bias was reduced if m was set to 2. It is almost impossible to estimate m directly from observed spectra because of small numbers of large drops sampled in a finite time. It seems that taking an exponential function, or even a single value of m in a gamma distribution, is not a sufficiently accurate way of parameterizing the drop size distribution in the range of diameters in which the radar parameters have the most weight—that is, where $N(D)D^6$ is greatest.

The fact that drop size distribution uncertainty severely limits the interpretation of Z in terms of rainfall rate is well known. Jameson (1991) showed that Z is the worst radar parameter at estimating the rainfall rate R in terms of the correlation between Z and R. The attenuation is the best radar parameter because it is almost insensitive to the many different drop size distributions that can have the same R. He further showed that a two-parameter (Z and Z_{DR}) calculation of R may be worse than using only one parameter if the experimental errors are too large ($\Delta Z > 0.5$ dB and $\Delta Z_{DR} > 0.1$ dB). Figure 9 reinforces these results.

Joss and Gori (1978) show that as the timescale of averaging increases drop size distributions tend to an exponential. The large-scale averaging, which is employed to obtain each point in Fig. 6, should have produced m values considerably nearer 0 if the entire drop size distribution over this area had been sampled at once. But many individual Z_{DR} and DDV measurements go into the average, each from a pulse resolution volume on the order of 100 m in each dimension. On this scale, the drop size distributions are not close to exponential, and the DDV and Z_{DR} measurements reflect this. These ''point'' measurements are averaged, and hence m is not close to the exponential value of zero. Measurements below this resolution cannot be performed by the radar, although it would be interesting to see whether the observed values of m change with resolution volume.

1) Effect of different drop shape expressions

Computed values of polarization parameters for rain are very sensitive to drop shapes. The modified Beard and Chuang shapes used above are slightly different from the semiempirical values of Pruppacher and Pitter (1971) and the analytic expression of Green (1975). We have calculated how the different drop shape expressions alter the theoretical DDV against Z_{DR} lines. In general, DDV is only a little decreased by using either Pruppacher and Pitter's shapes or Green's shapes, but there is a significant increase in Z_{DR}. This increase in Z_{DR} is due to the fact that the small particles are considered spherical for the modified Beard and Chuang shapes. This modification was made by Goddard et al. (1982) for the purpose of reducing the calculated Z_{DR} from a distrometer measurement of the drop size distribution so that it agreed with Z_{DR} simultaneously measured by a radar beam dwelling above the distrometer.

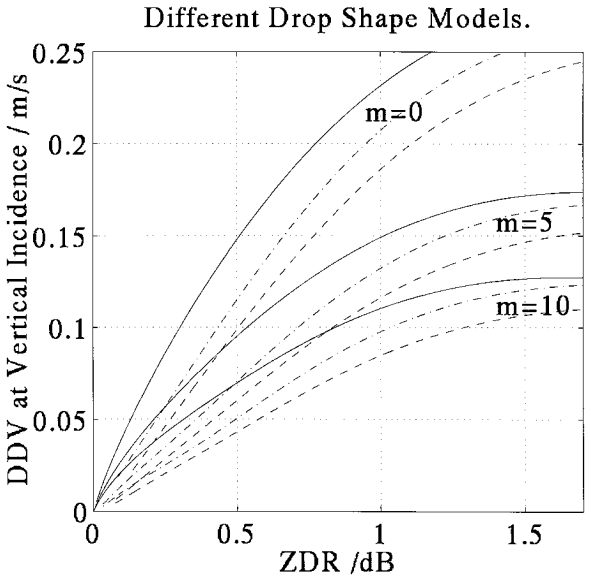

FIG. 10. Theoretical relationships between Z_{DR} (as if viewed at 0° elevation) and DDV for different models of drop shapes. The solid line represents the modified Beard and Chuang shapes given by Eq. (8), the chain dotted line the shapes of Pruppacher and Pitter, and the dashed line the shapes of Green.

Figure 10 shows the theoretical and measured values of DDV and Z_{DR} corresponding to Fig. 5, but for the Pruppacher and Pitter shapes, the Green shapes, and the modified Beard and Chuang shapes. Pruppacher and Pitter's shapes and Green's shapes give m values that are considerably lower for a measured value of DDV and Z_{DR}. Caution must be applied in the interpretation of values of m if there is any uncertainty concerning the drop shapes.

2) Sensitivity of DDV to different particle diameters

The D^6 backscattering powers mean that the reflectivity is most sensitive to the largest particles. The greatest contribution to rainfall rate comes from particles that have the largest value of $D^3 v_{fall}(D)$, which can be significantly smaller than those contributing to Z. One can perform a similar study for DDV (or any other radar

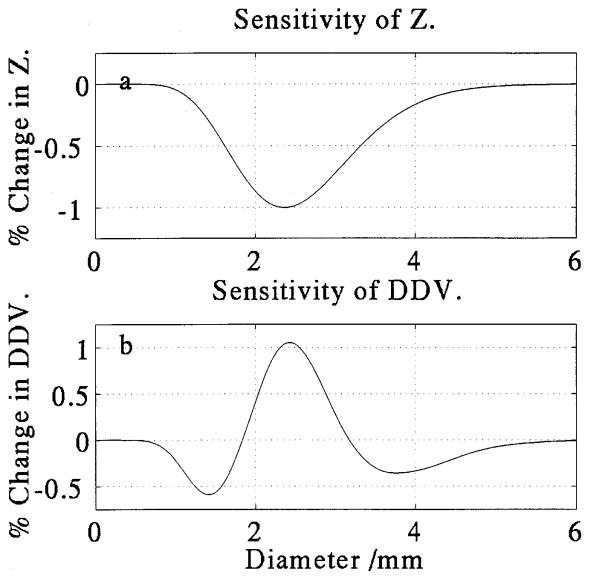

FIG. 11. (a) The sensitivity of Z to particle diameters is shown for an exponential drop size distribution with median diameter D_0 equal to 1.25 mm by considering the effect of removing all the particles in a diameter range of 0.02 mm; Z is most sensitive to particles with diameters of around 2.5 mm. (b) The corresponding plot for DDV showing the sensitivity to a broadly similar range of diameters.

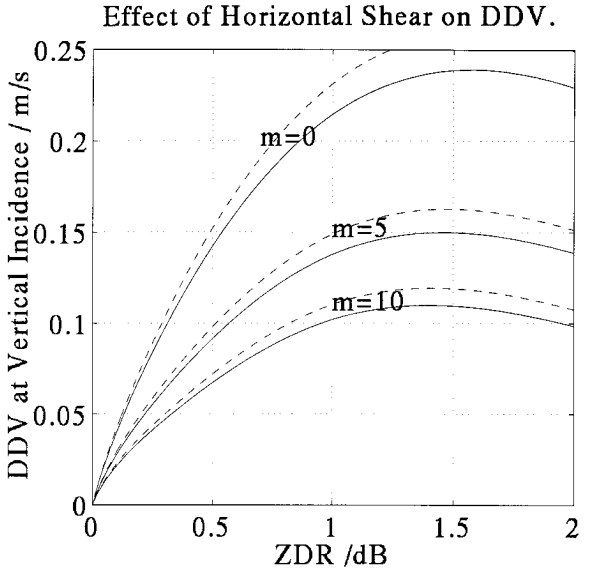

FIG. 12. The effect of 0.02-s^{-1} shear on the theoretical values of DDV made at 20° elevation angle. The solid lines represent the theoretical relationships when no shear is present. The dashed lines represent the relationship with 0.02-s^{-1} shear.

parameter) for a given distribution of particles by looking at the variation of DDV when all the particles in a particular size range (ideally infinitesimal) are removed from a calculation of DDV for that distribution. If DDV changes significantly, then it can be said to be sensitive to that size of particle. Figure 11 shows that for an exponential distribution, the greatest changes in DDV occur for particles of similar size to those that contribute to Z, although there is more contribution to DDV from both the smaller and larger particles. Hence, DDV and Z are sensitive to particles of similar sizes. This contrasts with rainfall rate, which is sensitive to smaller particles than Z. Hence, it can be assumed that a three-parameter fit of a gamma distribution performed by using DDV will still not fit particularly well to the drop sizes that actually contribute most to the rainfall rate. This is a problem with nearly all radar parameters.

3) WIND SHEAR AND DDV FOR RAIN

Using (7), it is simple to calculate the effect wind shear has on the measured DDV in rain. For a dwell at 20° and a shear level of 0.02 s^{-1}, which is fairly high but not unusual, the theoretical DDV against Z_{DR} lines are altered slightly, as demonstrated in Fig. 12. If the elevation angle is reduced or the shear is increased, then it becomes no longer possible to obtain quantitative information from DDV in rain; however, the amount of shear necessary for this is not common. All measurements should be checked to see if wind shear could be producing a significant effect. The results presented in this section are not significantly affected by shear, and the observation of different DDV values for the same Z_{DR} is valid.

4) EFFECT OF DROP OSCILLATIONS

It is worth considering the possible effects of drop oscillations. If the fall velocity of an oscillating drop remains constant regardless of its phase in the oscillation cycle, then a mean axial ratio identical to the one in the Z_{DR} calculation should be used. If drops fall faster when in their prolate orientation than in their oblate orientation, then this is equivalent to higher Z_{DR} particles falling more slowly, and so the measured DDV will be reduced. This will result in an inferred m that is higher. However, Illingworth and Caylor (1991) show, by using the copolar correlation coefficient, that the magnitude of oscillations is small. Hence, oscillations are unlikely to account for the difference in m values between those presented in this paper and those of Ulbrich and Atlas (1984).

b. Ice

The DDV in ice tends to be small, reflecting the fact that there is little spread of fall velocities. It is often slightly negative, with values between 0 and −0.05 m s^{-1}. Comparison of the measured DDV values with Z_{DR} shows that there is a distinct negative correlation between the DDV in ice and the Z_{DR}. This is shown in Fig. 13. The negative DDV implies that the slower-falling particles are more eccentric. This would be the case if these particles were pristine crystals and the

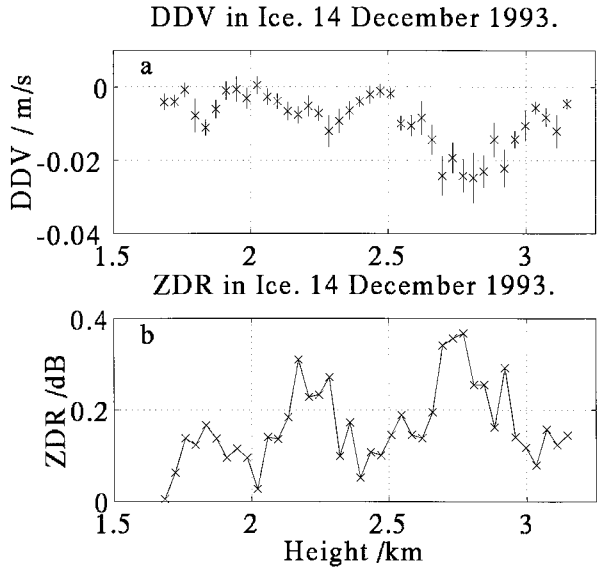

FIG. 13. (a) A measurement of DDV in ice made at 30° elevation angle. (b) The corresponding measurement of Z_{DR}. DDV is clearly seen to be correlated with Z_{DR}.

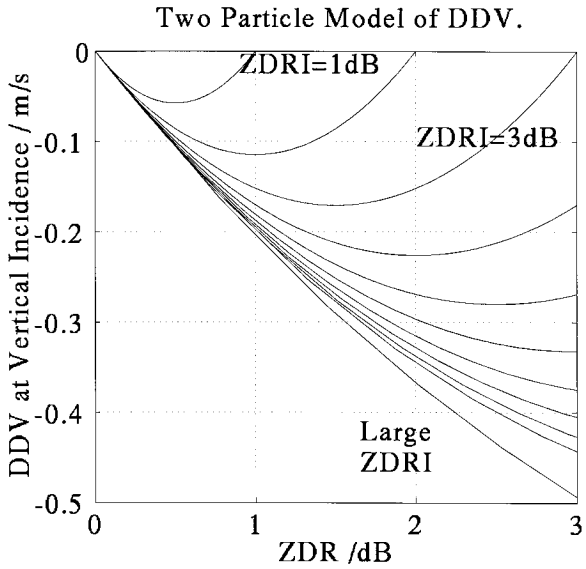

FIG. 14. Theoretical values of DDV and Z_{DR} for ice, assuming a model of spherical aggregates, eccentric crystals of a particular intrinsic Z_{DR}, and a fall velocity difference between them of 1 m s^{-1}. The curves represent different values of the Z_{DR} of the crystals, the distance along them representing the relative reflectivity-weighted proportions of crystals (right-hand side is all crystals) and aggregates (left-hand side is all aggregates).

larger particles were more spherical aggregates of the crystals. Very frequently the Z_{DR} of snow is very close to 0 dB, and hence it seems reasonable to presume that the largest of the aggregates are spherical. One can theoretically investigate the situation using published relationships between fall velocities, densities, and axial ratios of particles, such as given by Locatelli and Hobbs (1974), and study the behavior of DDV when the particle size distribution is altered. Consider a situation in which the reflectivity of the more spherical particles is greater than that of the more eccentric particles. Then additional eccentric particles will both increase Z_{DR} and, because there is a greater spread of Z_{DR} values, the magnitude of DDV. The important result is that, for a model in which axial ratios, densities, and fall velocities all vary smoothly in a physically reasonable way, the gradient of the magnitude of DDV with Z_{DR} is always less than about 25 mm s^{-1} dB^{-1}. This contrasts with measured gradients of around 30 to 70 mm s^{-1} dB^{-1}. This is a significant difference and is explained below.

Evidence exists from several sources, such as aircraft probe data (discussed by Thomason et al. 1995), that ice is best described by two distinct particle spectra. These are solid crystals with densities of 0.92 g cm^{-3} and aggregates with significantly smaller densities, typically of 0.05 g cm^{-3}. It is sensible to investigate such a two-component distribution with values of axial ratios chosen so that aggregates are considered spherical, whereas crystals are considered eccentric. Such a parameterization, using appropriate expressions from Locatelli and Hobbs (1974), can produce gradients of the order of those measured. This is further evidence for the two-component model. A further simplification of the DDV calculation can be performed as follows. Theoretically, it can be easily seen that any group of particles with the same Z_{DR} but different fall speeds can be considered as being equivalent to a single particle with that Z_{DR}. The reflectivity is equal to the reflectivity of the group of particles, and the fall velocity equal to the reflectivity-weighted mean fall velocity of the group of particles. Hence, assuming that all the crystals have the same Z_{DR}, one can simplify the situation of a spectrum of crystals and a spectrum of aggregates to just one crystal and one aggregate. This then allows analytic calculation of expected Z_{DR} and DDV values given a value of intrinsic Z_{DR} (Z_{DRI}—the Z_{DR} an individual particle would have if it was aligned with its long axis horizontal) for the crystals. One also requires a fall-speed difference between the crystals and the aggregates, and the relative reflectivities of the crystals and aggregates. Figure 14 displays the situation for a fall speed difference of 1 m s^{-1}. The left-hand side of each curve (where observations are expected to lie) represents the case in which nearly all aggregates are present (in terms of reflectivity). The right-hand side represents the case in which the particles are nearly all crystals. It is clear that, in order for there to be a negative correlation between Z_{DR} and DDV, the aggregates must have a higher reflectivity than the crystals. Also, as the number of crystals becomes small, the relationship between the measured Z_{DR} and DDV becomes independent of the Z_{DR} of the crystals and tends toward a straight line. This is suggested by the observations. The gradient of DDV and Z_{DR} can be thus used to infer a velocity difference between the aggregates and the crystals. Figure 14 pre-

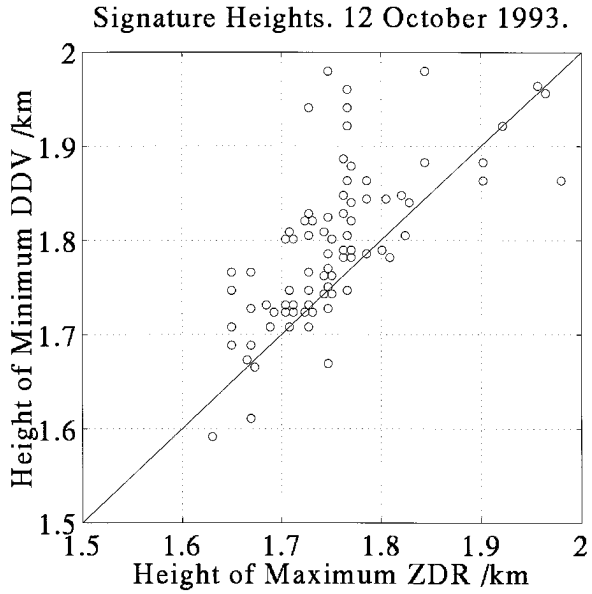

FIG. 15. Altitudes of the maximum Z_{DR} and minimum DDV in the melting layer.

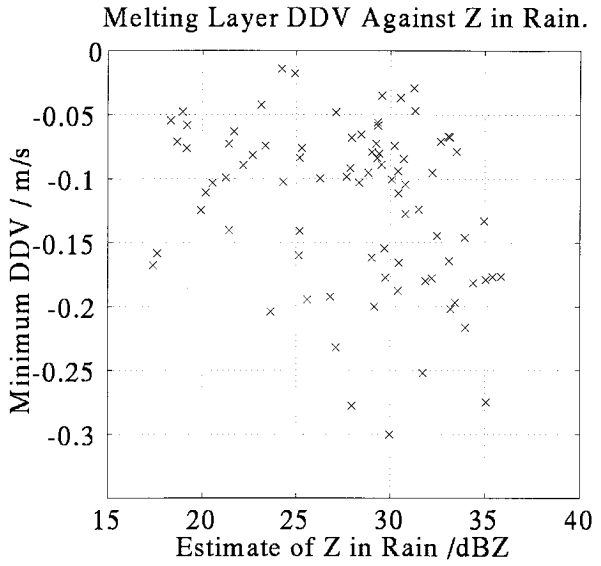

FIG. 16. The minimum DDV in the melting layer against the reflectivity in the rain (from a large-angle PPI at 15° elevation). The minimum DDV values decrease as Z increases.

dicts a gradient of 200 mm s^{-1} dB^{-1}, about four times larger than observations, suggesting that fall velocity differences are at least 0.25 m s^{-1}. When one realizes that the crystals must have a positive fall velocity, this provides a lower limit to the fall velocity of the aggregates.

Hence, DDV can be used to suggest that a single, smoothly varying spectrum of particles is not a good way of describing the ice. A minimum fall speed can also be deduced. It is possible that DDV can be used to follow the progress of aggregation.

c. The melting layer

As was the case for ice, no particular relationship is expected within the melting layer between fall velocity and the Z_{DR} of particles. The negative DDV measurements, suggested by Fig. 4, show that the faster-falling particles are more spherical. The obvious interpretation for this is that these particles are fully melted raindrops, whereas the more eccentric particles are partially melted snowflakes. The partially melted snowflakes are falling more slowly due to their larger cross-sectional area. A survey of measurements within the melting layer reveals a number of points. First, the altitude of the minimum value of DDV in the melting layer is equal to, or above, the altitude of the maximum Z_{DR} in the melting layer, shown in Fig. 15. Second, the magnitude of the minimum DDV has a weak dependence upon the rainfall rate of the event. The higher the rainfall rate is, the higher the magnitude of DDV (Fig. 16). This can be explained by the fact that higher rainfall rates generally contain particles with larger fall velocities. This will increase the magnitude of any measured DDV. Third, Fig. 17 shows that the magnitude of the minimum DDV depends upon the maximum Z_{DR} in the melting layer. Again, this is not too surprising; if the slowly falling snowflakes become more eccentric, then Z_{DR} will rise, and since there is a greater difference between the weight that the snowflakes contribute to v_H and v_V, the magnitude of DDV will increase as well.

Unfortunately, theoretical models of what is occurring require the use of an advanced melting-layer model capable of calculating axial ratios of particles as well as the normal parameters derived in these models, such as

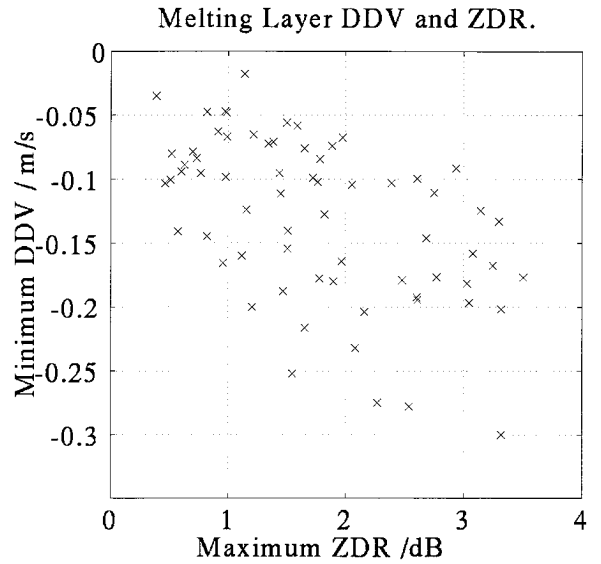

FIG. 17. The minimum DDV in the melting layer against the maximum Z_{DR} in the melting layer. The two show some correlation.

fall velocities and densities. The authors have written such a model, although its complete description is outside the scope of this paper, but we are unable to reproduce the observed negative peak in DDV without an unrealistic fall velocity parameterization.

Quantitative inferences are hard to draw from the melting layer, although one can proceed a little way by drawing on the two-component model discussed for ice. Measurements are also harder to perform; since the copolar correlation coefficient ρ falls in the melting layer, the correlation between the values of v_H and v_V also falls, and the statistical error in the value $v_H - v_V$ increases.

5. Variations of DDV

a. Combined differential Doppler velocity

The Chilbolton radar transmits alternately horizontally and vertically polarized radiation, so there is a third estimate of the Doppler velocity, v_{HV}. This is performed by correcting the phase of the return from the vertically polarized pulses for any differential propagation phase shift $\phi_{\rm DP}$ and then calculating a Doppler velocity using the combined time series. For the standard estimation of Doppler velocities, this has the advantage that the effective pulse repetition frequency has doubled, and therefore the folding velocity of the estimate has also doubled. It would be reasonable to presume that v_{HV} lies midway between v_H and v_V. However, this is not necessarily the case, as measurements and theoretical calculations both show.

Theoretically, for calculating the velocity v_{HV}, one needs to consider the power-weighted velocity distribution given by

$$v_{HV} = \frac{\sum |S_{hi}||S_{vi}|v_i}{\sum |S_{hi}||S_{vi}|}, \tag{9}$$

where v_i is the Doppler velocity of the ith particle, $|S_{hi}|$ is the square root of the reflectivity of the ith particle in the horizontal polarization, and $|S_{vi}|$ is the square root of the reflectivity in the vertical polarization.

This means that a group of particles (at a particular fall velocity) that has a spread of different values of $|S_{vi}|$ for each $|S_{hi}|$ (i.e., a low correlation coefficient ρ) contributes less weight to v_{HV} than it does to both v_H and v_V. Hence, the estimate of v_{HV} need not be the average of v_H and v_V. We define a quantity, which we call DDV$_{HV}$, as

$$\text{DDV}_{HV} = \frac{2(v_H - v_{HV})}{\sin\theta}, \tag{10}$$

which, if v_{HV} does equal the mean of v_H and v_V, will be equal to DDV. Qualitatively, if DDV$_{HV}$ is larger than DDV, then the faster-falling particles have a lower correlation coefficient than the slower-falling ones and vice versa. Theoretical calculations for rain show that DDV$_{HV}$ exceeds DDV by only a few percent, which is too small to measure, and there is no new information contained in this parameter. Figure 18 shows a ray of DDV and DDV$_{HV}$, demonstrating that in the melting layer, DDV$_{HV}$ can be slightly smaller than DDV. This indicates that the low correlation coefficient comes from the more slowly falling particles. These have already been identified as eccentric, partially melted snowflakes. Normally, DDV$_{HV}$ is indistinguishable from DDV in ice. Figure 18 shows that, at high altitudes, DDV$_{HV}$ can sometimes become positive (around $+0.02$ m s^{-1}), while DDV remains negative (around -0.01 m s^{-1}). This implies that the velocity v_{HV} is less than both v_H and v_V, and suggests that the fastest-falling particles have low values of the correlation coefficient. This is in conflict with the assumption that the fastest-falling particles are spherical aggregates that will have high values of the correlation coefficient. It is not clear what is occurring in this example, and an explanation for the inconsistency has not been found.

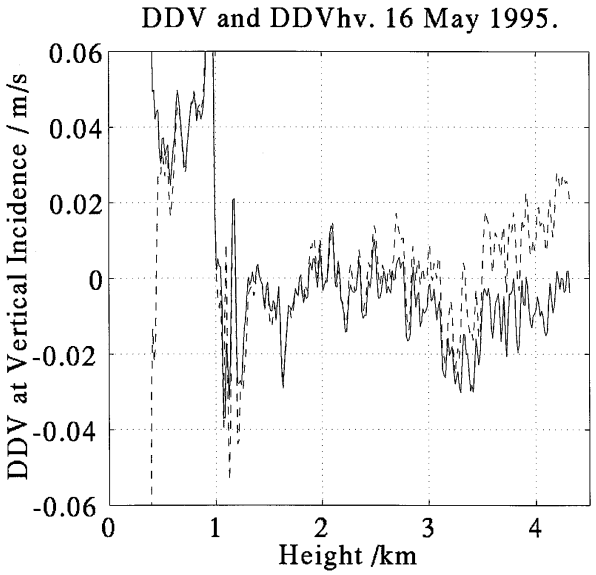

FIG. 18. A ray taken at 10° elevation of DDV (solid) and DDV$_{HV}$ (dashed) in rain, the melting layer, and ice. At altitudes above 3 km, DDV$_{HV}$ becomes significantly higher than DDV.

b. Cross-polar differential Doppler velocity

Another variant of DDV exists. The Chilbolton radar can also record the time series of the cross-polar return. A Doppler velocity can be found for this time series (corresponding to horizontally polarized transmitted pulses) in precisely the same way as for a copolar time series. The power frequency spectrum for the cross-polar return is composed of two parts. The Doppler velocity of the precipitation particles will produce power at the corresponding frequency, but this spectrum will be convoluted by a width that is produced due to the rocking of the particles. The faster the particles rock, the larger the width will be. The rocking will not affect the mean value of the Doppler velocity v_x, which will

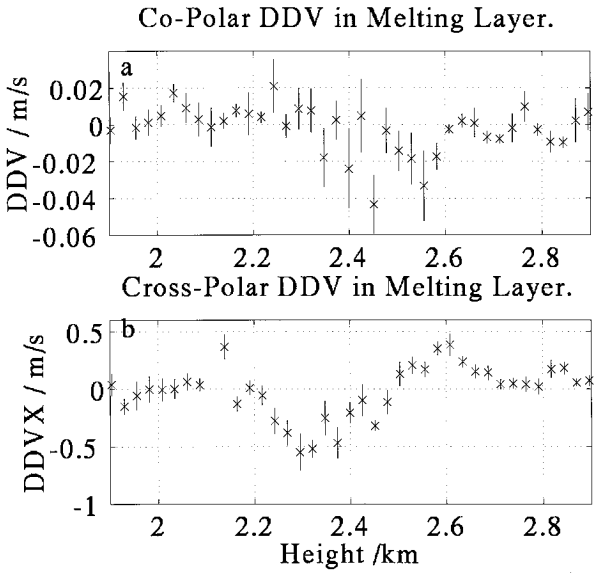

FIG. 19. (a) A ray of DDV for a melting layer in light precipitation. (b) The corresponding value of DDVX.

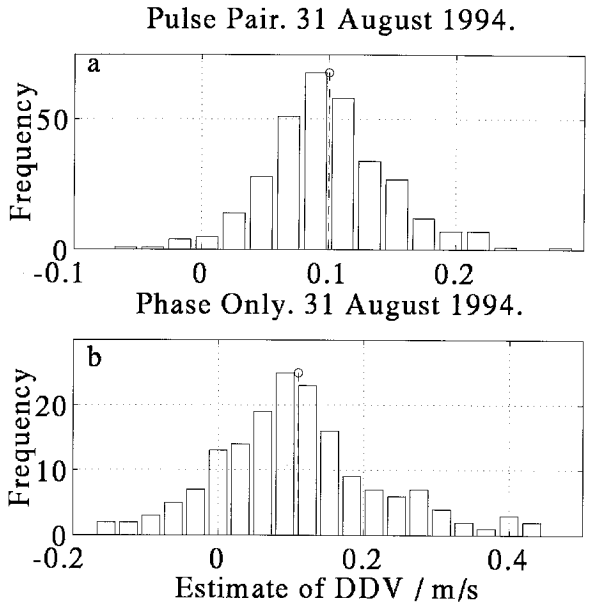

FIG. 20. (a) Actual estimation of DDV in rain from 128 pulse-pair time series for the pulse-pair estimator. (b) The same estimation but using the phase-only estimator. The circle marks the mean value in each case.

be identical to v_H if all the particles have the same linear depolarization ratio (LDR). Hence, another differential Doppler velocity can be defined as

$$\mathrm{DDVX} = \frac{v_H - v_X}{\sin\theta}, \tag{11}$$

which will be negative if the faster-falling particles contribute most to the depolarization or positive if the slower-falling particles contribute most to the depolarization. Obviously, such a measurement can only be performed where there is high LDR and the cross-polar return has a high signal to noise ratio. This restricts any meaningful results for the melting layer or high-LDR ice. Few measurements of this quantity have been performed. Initial results suggest that the magnitude of DDVX can be up to ± 0.5 m s^{-1} (Fig. 19), which is much greater than the magnitude for DDV. These larger values arise because there can be large differences in LDR across a spectrum, while only much smaller changes in Z_{DR} can occur. Its sign appears to change within the melting layer from positive just after the onset of melting to negative near the end of melting. The negative DDVX does not agree with the simple idea that the melting layer can be treated as containing slowly falling, partially melted, depolarizing particles and faster-falling, fully melted raindrops. This would give $v_X < v_H$ and, hence, positive DDVX. Further observations may reveal the processes that are occurring. It is possible that the DDVX parameter can also reveal more information about the nature of dry ice particles.

6. Measurement accuracy

This section briefly summarizes the empirically observed accuracies of the DDV measurement and suggests some observing strategies. Obviously, the longer the observation is, the lower the error in the measurement. It is observed that the error in a single measurement of DDV reduces in accordance with the standard statistical result; that is, the error is proportional to the inverse square root of the observing time. Empirically, for a dwell time of 7 s (around 2000 pulse pairs for the Chilbolton radar), the data gives an error in $v_H - v_V$ in rain of roughly 0.003 m s^{-1}. At an elevation angle of 20°, this corresponds to an error in DDV of around 0.01 m s^{-1}, as shown in Fig. 4. The magnitude of the error in ice is significantly less than this because of the reduced spectral width, although the fractional error is greater, since DDV is closer to zero. Errors can also be reduced by averaging over several range gates, as demonstrated in Fig. 7, as long as the spatial variation of the parameters is small over the averaging range. The errors restrict the use of measuring DDV to dwells or slow scans; a scan rate of 1° s^{-1} for the Chilbolton radar (0.25 s per beamwidth) is not sufficiently slow unless large-scale averaging takes place. Figure 20 shows the distribution of DDV estimates made using 128 pulse-pair (0.4 s) samples in rain from a region where the true DDV did not change significantly. This figure indicates the spread of DDV values likely from only a short length of time series.

If one has recorded a long time series, it is best to average the DDV measurements produced by different sections of the series (around 1-s sections) rather than using the series as a whole. This is because of the possibility that the mean Doppler wind speed has increased over the interval, which will be obviously more likely

if the radar is scanning. The longer time series will thus have a large spectral width, which, as described in section 3, increases the error in the DDV measurement.

Since the variation of Doppler velocity due to the wind shear is a potential cause of problems for the DDV measurement, one may presume that measurements along a ray that is at right angles to the wind direction will be better than those aligned with the wind. We have searched for this effect in our data, but it appears not to be significant. Hence, for the Chilbolton radar, no account of the wind direction needs to be made when forming a measurement sequence.

It is desirable to be able to record DDV in an RHI (range–height indicator) scanning mode. Observations show that this is not easy to do. Empirically, a scan rate of around 0.25° s^{-1} is required to reduce the sample errors to a reasonable level, and the minimum elevation angle at which DDV can be reasonably estimated is around 7°. Shear effects are enhanced by vertical scanning since the effective width of the beam is increased. For accurate measurements, dwells are best. If a region needs to be studied, PPIs can be taken.

7. Conclusions

The differential Doppler velocity, defined as the difference between Doppler velocities measured at horizontal and vertical polarization, can be used to obtain information about precipitation systems that is unavailable by other methods. DDV in rain can be used in conjunction with Z and Z_{DR} to produce a three-parameter gamma fit to the drop size distribution. It gives m values of around 2–11, with 5 being a typical mean. These values are sensitive to drop shapes and could be affected by oscillations. Illingworth and Caylor (1991) show, however, that the magnitude of oscillations is small. DDV weights the particles of similar size to those affecting Z and Z_{DR}, whereas calculations based around measurements of rainfall rates weight smaller particles. A value of $m = 5$ is consistent with Goddard and Cherry (1984).

There is a spread of DDV values for the same Z_{DR}, which indicates that it is impossible to accurately parameterize the drop size distribution in terms of only two parameters. The variations of m from 2 to 11 suggest a spread in rainfall rates of ±15% about a value calculated from Z and Z_{DR}, assuming that $m = 5$. This implies that natural variations in the drop size distribution will mean that radar measurement of rainfall rates to better than 15% accuracy will be extremely difficult. This is a fundamental limit on the accuracy with which a radar can measure precipitation rates using reflectivity-based observations.

In ice, DDV suggests the existence of two different particle types: eccentric, slowly falling crystals and electromagnetically spherical aggregates falling at least 0.25 m s^{-1} faster. It is postulated that changes of Z_{DR} and Z, which are often observed in an RHI, may be due to changes in the proportion of crystals and aggregates present rather than any changes in the type of particles. Use of a theoretical model based on a smoothly varying drop size distribution, particle density, and fall speed with diameter cannot reproduce the large magnitudes of DDV observed for a given Z_{DR}. Accurate measurements of DDV may perhaps be able to follow the conversion of crystals to aggregates.

In the melting layer, DDV shows that the faster-falling particles are more spherical. It is likely that these are fully melted raindrops, whereas the more slowly falling particles are partially melted, eccentric snowflakes. DDV is difficult to assess within the melting layer because of the complex processes and particle distributions that occur. There is also an increased noisiness to the estimator. Perhaps, however, DDV and other polarization parameters in the melting layer may lead to a better understanding of the melting process.

DDV is independent of turbulence and, in many cases, shear. This is its major advantage over similar techniques. It is more reliable if the beamwidth of the radar is narrow. It can be measured on any dual-polarization Doppler radar, whether the time series of the individual amplitudes and phases are recorded for postprocessing (as at Chilbolton) or calculations of Doppler velocity are performed on-line.

Acknowledgments. We would like to thank RCRU at RAL for the use of the Chilbolton radar. One of us (DRW) acknowledges the support of a Gassiot scholarship. This research was funded by NERC Grants GR3/8523 and GST/02/718.

APPENDIX

The Independence of DDV with Respect to Turbulence

Section 3 allows one to calculate DDV as the difference in the velocities v_H and v_V given by the integrals

$$\bar{v}_H = \frac{\int_{v=-\infty}^{\infty} H(v) v \, dv}{\int_{v=-\infty}^{\infty} H(v) \, dv} \tag{A1}$$

(and similarly for v_V), where $H(v)$ is the power spectrum in the horizontal polarization caused by the fall velocities of the particles as a function of their Doppler velocity v. The effect on v_H if the power spectrum H is convoluted by a spectrum C (representing turbulence) is shown below.

First, consider the power spectrum as a function of velocity when there is turbulence present. The power spectrum $H_c(v)$ can be written as

$$H_c(v) = \int_{u=-\infty}^{\infty} C(v - u) H(u) \, du, \tag{A2}$$

which means that the mean velocity in the presence of turbulence v_{H_c} can be written as

$$\bar{v}_{H_c} = \frac{\int_{v=-\infty}^{\infty}\int_{u=-\infty}^{\infty} C(v-u)H(u)v\,du\,dv}{\int_{v=-\infty}^{\infty}\int_{u=-\infty}^{\infty} C(v-u)H(u)\,du\,dv}. \quad \text{(A3)}$$

It is necessary to compare this quantity to that in (A1). One can proceed by a variable change. By writing $w = v - u$ and integrating in terms of w and u, so $dw = dv$, one can rewrite (A3) as

$$\bar{v}_{H_c} = \frac{\int_{w=-\infty}^{\infty}\int_{u=-\infty}^{\infty} (w+u)C(w)H(u)\,du\,dw}{\int_{w=-\infty}^{\infty}\int_{u=-\infty}^{\infty} C(w)H(u)\,du\,dw}. \quad \text{(A4)}$$

One now can split the double integral into separate u parts and v parts as follows:

$$\bar{v}_{H_c} = \frac{\int_{w=-\infty}^{\infty} C(w)w\,dw \int_{u=-\infty}^{\infty} H(u)\,du + \int_{w=-\infty}^{\infty} C(w)\,dw \int_{u=-\infty}^{\infty} H(u)u\,du}{\int_{w=-\infty}^{\infty} C(w)\,dw \int_{u=-\infty}^{\infty} H(u)\,du}. \quad \text{(A5)}$$

Hence one can write (A5) as a sum of two parts,

$$\bar{v}_{H_c} = \bar{w}_c + \bar{v}_H, \quad \text{(A6)}$$

where v_H is the mean Doppler velocity of the power distribution H unaffected by turbulence and w_c is a modifier equal to

$$\bar{w}_c = \frac{\int_{w=-\infty}^{\infty} C(w)w\,dw}{\int_{w=-\infty}^{\infty} C(w)\,dw}. \quad \text{(A7)}$$

This is independent of the power distribution H; w_c will equal 0 if $C(w)$ is symmetrical about $w = 0$, although this is not necessary to continue the argument. A similar analysis for power in the vertical polarization will reveal that

$$\bar{v}_{V_c} = \bar{w}_c + \bar{v}_V, \quad \text{(A8)}$$

and hence their subtraction, which should be equal to DDV in the presence of turbulence, will be equal to

$$\text{DDV}_c = \bar{v}_{H_c} - \bar{v}_{V_c} = \bar{v}_H - \bar{v}_V = \text{DDV}, \quad \text{(A9)}$$

thus showing the independence of turbulence on DDV. This derivation is independent of the form of the convolution C, although the actual estimator of DDV by pulse pairs may be slightly affected.

REFERENCES

Beard, K. V., and C. Chuang, 1987: A new model for the equilibrium shape of raindrops. *J. Atmos. Sci.,* **44,** 1509–1524.

Doviak, R. J., and D. S. Zrnić, 1984: *Doppler Radar and Weather Observations.* Academic Press, 458 pp.

Goddard, J. W. F., and S. M. Cherry, 1984: Quantitative precipitation measurements with dual linear polarization radar. Preprints, *22d Conf. on Radar Meteorology,* Zurich, Switzerland, Amer. Meteor. Soc., 352–357.

——, ——, and V. N. Bringi, 1982: Comparison of dual-polarization radar measurements of rain with ground-based disdrometer measurements. *J. Appl. Meteor.,* **21,** 252–256.

Green, A. W., 1975: An approximation for the shapes of large droplets. *J. Appl. Meteor.,* **14,** 1578–1583.

Gunn, R., and G. D. Kinzer, 1949: The terminal velocity of fall for water droplets in stagnant air. *J. Meteor.,* **6,** 243–248.

Illingworth, A. J., and I. J. Caylor, 1991: Co-polar correlation measurements of precipitation. Preprints, *25th Int. Conf. on Radar Meteorology,* Paris, France, Amer. Meteor. Soc., 650–653.

Jameson, A. R., 1991: A comparison of microwave techniques for measuring rainfall. *J. Appl. Meteor.,* **30,** 32–54.

Joss, J., and E. G. Gori, 1978: Shapes of raindrop size distributions. *J. Appl. Meteor.,* **17,** 1054–1061.

Locatelli, J. D., and P. V. Hobbs, 1974: Fall speeds and masses of solid precipitation particles. *J. Geophys. Res.,* **79,** 2185–2197.

Marshall, J. S., and W. M. K. Palmer, 1948: The distribution of raindrops with size. *J. Meteor.,* **5,** 165–166.

Metcalf, J. I., 1986: Interpretation of the autocovariances and cross-covariance from a polarization diversity radar. *J. Atmos. Sci.,* **43,** 2479–2498.

Poiares Baptista, J. P. V., 1994: *OPEX Workshop.* Vol. 4, *Reference Book on Radar.* ESA, 104 pp.

Pruppacher, H. R., and R. L. Pitter, 1971: A semi-empirical determination of the shape of cloud and raindrops. *J. Atmos. Sci.,* **28,** 86–94.

——, and J. D. Klett, 1978: *Microphysics of Clouds and Precipitation.* D. Reidel Publishing, 714 pp.

Russchenberg, H. W. J., 1993: Doppler polarimetric radar measurements of the gamma drop size distribution of rain. *J. Appl. Meteor.,* **32,** 1815–1825.

Thomason, J. W. G., A. J. Illingworth, and V. Marécal, 1995: Density and size distribution of aggregating snow particles inferred from coincident aircraft and radar observations. Preprints, *27th Conf. on Radar Meteorology,* Vail, CO, Amer. Meteor. Soc., 127–129.

Ulbrich, C. W., 1983: Natural variations of the analytic form of the raindrop size distribution. *J. Climate Appl. Meteor.,* **22,** 1764–1775.

——, and D. Atlas, 1984: Assessment of the contribution of differential polarization to improved rainfall measurements. *Radio Sci.,* **19,** 49–57.